Selective oxidation of sulfides and hydrocarbons with H_2O_2 over manganese catalyst supported on nanoparticles

Massomeh GHORBANLOO[1,*]**, Roghayeh TARASI**[1]**,**
Jun TAO[2]**, Hidenori YAHIRO**[3]
[1]Department of Chemistry, Faculty of Science, University of Zanjan, Zanjan, Iran
[2]State Key Laboratory of Physical Chemistry of Solid Surfaces and Department of Chemistry, College of Chemistry
and Chemical Engineering, Xiamen University, Xiamen, Fujian Province, P. R. China
[3]Department of Applied Chemistry, Faculty of Engineering, Ehime University, Matsuyama, Japan

Abstract: A new magnetically separable catalyst consisting of binuclear Mn(II) complex $[Mn_2(HL)_2(H_2O)_4]$, HL = 2-[(2-hydroxy-benzylidene)-amino]-3-(4-hydroxyphenyl)-propionic acid, supported on (3-chloropropyl)-trimethoxysilane (CPTMS) functionalized silica-coated magnetic nanoparticles (MNPs) was prepared. The synthesized catalyst was characterized by several physico-chemical and spectroscopic methods. This immobilized complex was found to be an efficient heterogeneous catalyst for the oxidation of different sulfides and hydrocarbons using hydrogen peroxide (H_2O_2) as an oxidant. The catalyst is readily recovered by simple magnetic decantation and can be recycled several times with no considerable loss of catalytic activity.

Key words: Magnetic, heterogeneous catalyst, binuclear, nanoparticles, oxidation, H_2O_2

1. Introduction

Nanomagnetic systems have been extensively used in biomedical and pharmaceutical applications.[1] Magnetic nanoparticles (MNPs) of iron oxides have attracted much attention because of their unique properties and potential applications in different fields, such as magnetically assisted drug delivery and magnetic resonance imaging (MRI) contrast agents.[2] Moreover, MNPs are good supports for immobilization of homogeneous catalysts.[3] Therefore, catalytic systems with MNP supports have been successfully utilized in catalyzing a broad series of chemical reactions such as oxidation[4] and polymerization.[5]

The oxidation of organic sulfides to the corresponding sulfoxides is one of the essential functional group transformations in organic synthesis.[6] Organic sulfoxides are important synthetic intermediates for the production of chemically and biologically active molecules and also show promise as remedial agents.[7]

Catalytic oxidation of hydrocarbons is also of great importance in the chemical industry for the exchange from petroleum-based feed stocks to valuable chemicals such as diols, epoxides, alcohols, and carbonyl compounds.[8] For example, benzaldehyde, a characteristic product of toluene oxidation, and aromatic ketones are very important starting materials for the preparation of intermediates in perfumery and pharmaceuticals.[9] Production of aromatic ketones by Friedel–Crafts acylation of aromatics leads to the production of toxic and corrosive wastes. Lately, there has been increased attention on finding clean, economical catalytic processes for synthesizing ketones via benzylic oxidation of alkyl aromatics.[10]

---

*Correspondence: m_ghorbanloo@yahoo.com

There are several oxidants such as hydrogen peroxide (H_2O_2), *tert*-butylhydroperoxide (TBHP), and iodosylbenzene (PhIO) for oxidation. However, H_2O_2 is regarded as a perfect 'green' oxidant, because of its absence of toxic by-products. Hence, robust, efficient, and recyclable heterogeneous catalysts have been developed for activation of H_2O_2 for oxidation of substrates Heterogeneous oxidation catalysts are notable, due to their easy handling, product separation, catalyst recovery, and reduced waste. Fixation of such complexes by covalent attachment to a functionalized support provides stable heterogeneous catalysts.[11] For this purpose, MNPs are potential candidates, and catalytic systems based on super-paramagnetic nanoparticles as a support have been discussed.[12,13] One of the major advantages of a catalytic system anchored in MNPs is that they can be well isolated by a simple magnetic separation procedure. However, MNPs have a tendency to aggregate in liquid media owing to their magnetic dipole–dipole interaction,[3] and so their surface area and magnetism may be decreased. Therefore, coating with a thin layer of silica has been used to stabilize bare MNPs to avoid their agglomeration in solutions.[3] Silica is one of the best materials for coating of MNPs because of its high chemical stability and easy functionalization.[14−16] There are numerous reports on the preparation and applications of silica-coated MNPs.[17−19]

In this work, the catalytic performance of $Fe_3O_4@SiO_2/([Mn_2L(HL)(H_2O)_4]$ was checked by sulfide and hydrocarbon oxidation with 30% aqueous H_2O_2. We also compared the catalytic activity of our earlier reported catalysts[20] and $Fe_3O_4@SiO_2/([Mn_2L(HL)(H_2O)_4])$ catalyst in the oxidation of methyl phenyl sulfide.

2. Results and discussion

2.1. Synthesis and immobilization

The Schiff base ligand H_3L was synthesized by the condensation of salicylaldehyde with L-tyrosine in 1:1 molar ratio in methanol.[21] Its manganese complex was synthesized and characterized according to our previously reported method[20] (Scheme 1).

The complex was immobilized on SiO_2-coated magnetite nanoparticles using (3-chloropropyl)-trimethoxy-silane as a linker. Immobilization of the complex involves reaction of their phenolic groups with (3-chloropropyl)-trimethoxysilane (CPTMS) (Scheme 1). The CPTMS moiety is bonded strongly to $Fe_3O_4@SiO_2$ by means of a covalent bond that prevents/reduces leaching of the catalyst in polar solvents. We washed these compounds to ensure that only the covalently attached molecules remained on the support.

2.2. Characterization

The FTIR spectrum of H_3L ligand is shown in Figure 1. There are no bands at 3245 and 1745 cm^{-1} due to the $\upsilon(NH_2)$ group of amino acids and $\upsilon(C=O)$ of salicylaldehyde, respectively. In its place, a new important band at 1613 cm^{-1} owing to azomethine $\upsilon(C=N)$ linkage appeared in this ligand.[21]

Figure 2 shows the FTIR spectra of the heterogeneous compounds: Fe_3O_4, $Fe_3O_4@SiO_2$, and $Fe_3O_4@SiO_2/[Mn_2L(HL)(H_2O)_4]$. The FTIR spectrum of Fe_3O_4 (Figure 2a) exhibited the expected Fe–O stretching absorption at 580 cm^{-1}. This peak appears in all the IR spectra of heterogeneous compounds, which are assigned to the Fe–O group. In IR spectra of the Fe_3O_4/SiO_2 and $Fe_3O_4@SiO_2/[Mn_2L(HL)(H_2O)_4]$, the absorption intensity of the Fe–O group decreases with the addition of the silica portion[22] and a strong absorption intensity of the Si–O–Si group appears owing to the silica coat. In Figure 2b, the bands at 477, 950, and 1098 cm^{-1} are assigned to $\delta(Si–O–Si)$, $\nu(Si–OH)$, and $\nu_{as}(Si–O–Si)$, respectively.[23]

The FTIR spectrum of the supported catalyst, $Fe_3O_4@SiO_2/[Mn_2L(HL)(H_2O)_4]$ (Figure 2c), exhibits
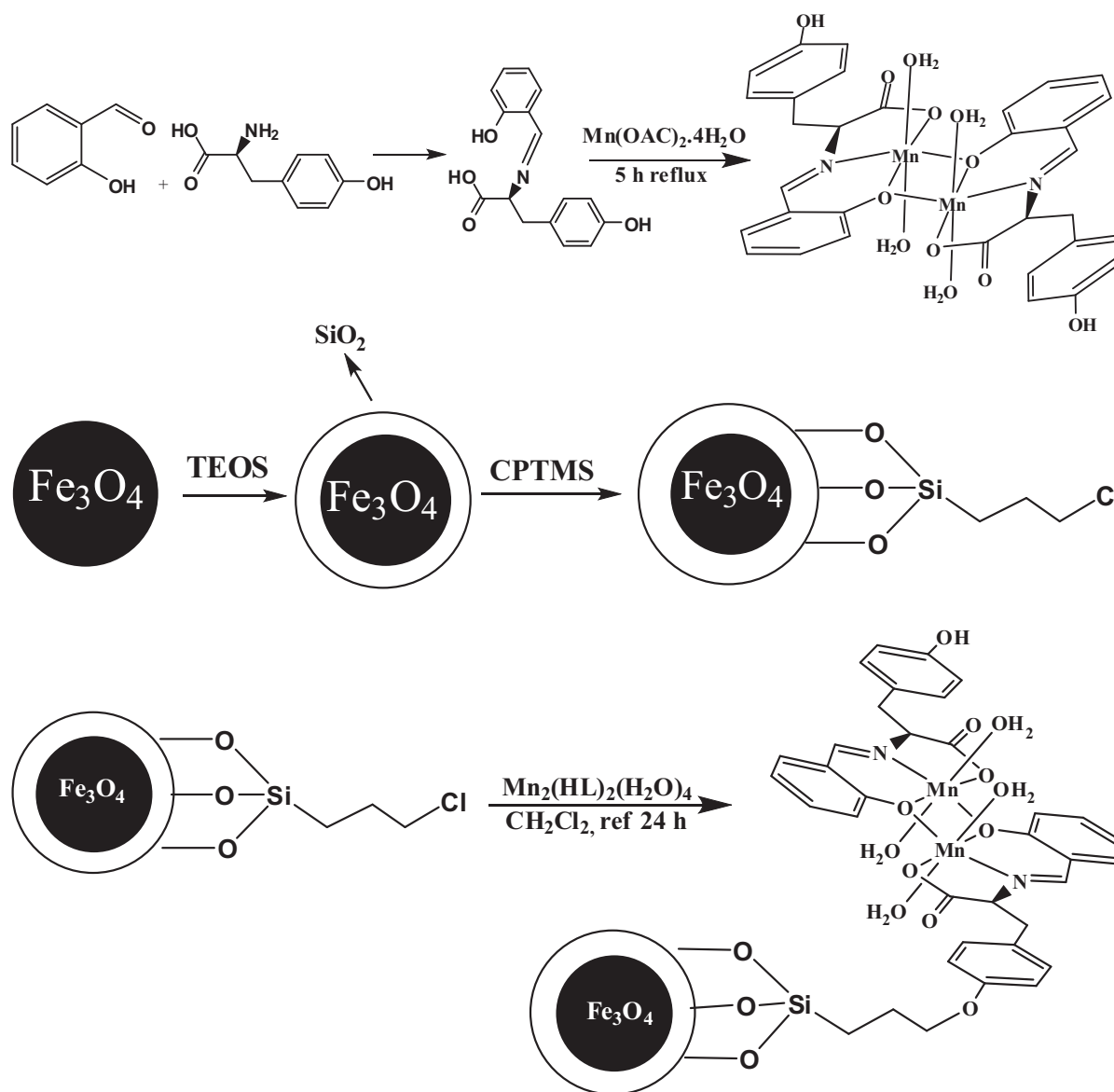
Scheme 1. Schematic representation of the formation of $e_3O_4@SiO_2/[Mn_2L(HL)(H_2O)_4]$.

the new characteristic bands of the complex units at 1647 (C=N), 1596 (ν_{as}(COO)), 1388 (ν_s(COO)), $\sim$400, and $\sim$530 cm^{-1} υ(M–N) and υ(M–O) associated with silica matrix bands at 1097, 809, and 477 cm^{-1} and magnetite matrix band at $\sim$580 cm^{-1}. Typically, a broad band with high intensity in the range of 3500–3400 cm^{-1} corresponded to the O–H vibration of SiO–H groups and HO–H of adsorbed water.[24] Hence, the FTIR characterization confirmed the successful immobilization of the Mn(II) complex to the modified $Fe_3O_4@SiO_2$ nanoparticles.

The morphologies of Fe_3O_4, $Fe_3O_4@SiO_2$, and $Fe_3O_4@SiO_2/[Mn_2L(HL)(H_2O)_4]$ were characterized with scanning electron microscopy. As shown in Figure 3, the nanoparticles sizes of Fe_3O_4, $Fe_3O_4@SiO_2$, and $Fe_3O_4@SiO_2/[Mn_2L(HL)(H_2O)_4]$ were about 18, 39, and 63 nm, respectively. Moreover, as it is shown, these nanoparticles had spherical shapes.
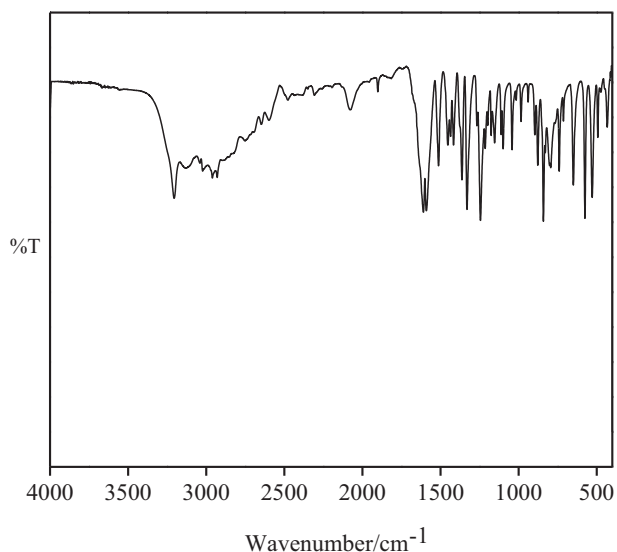
Figure 1. FTIR spectrum of H_3L.
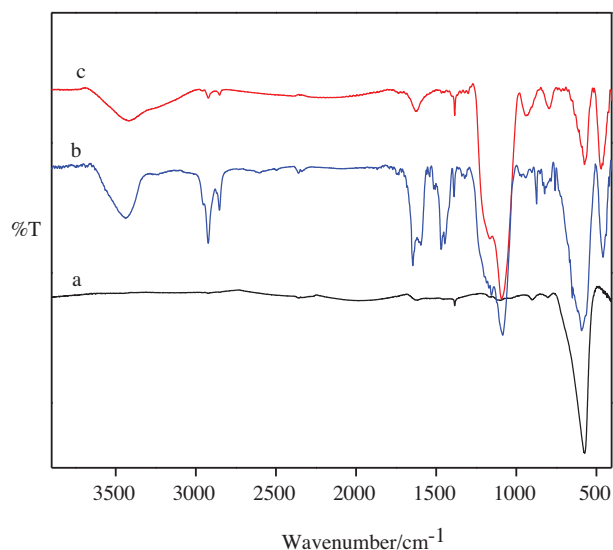
**Figure 2.** FTIR spectra of a) Fe_3O_4, b) $Fe_3O_4@SiO_2/[Mn_2L(HL)(H_2O)_4]$, c) $Fe_3O_4@SiO_2$.
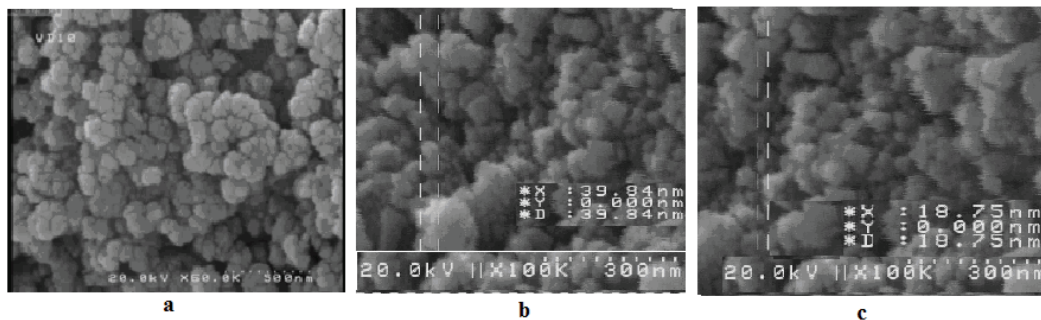
Figure 3. SEM image of a) $Fe_3O_4@SiO_2/[Mn_2L(HL)(H_2O)_4]$, b) $Fe_3O_4@SiO_2$, c) Fe_3O_4.

Magnetization data for Fe_3O_4, $Fe_3O_4@SiO_2$, and $Fe_3O_4@SiO_2/[Mn_2L(HL)(H_2O)_4]$ were collected between –5 and +5 T at room temperature and the M versus H curves are shown in Figure 4. All samples show super-paramagnetic properties, indicating the retaining of the nanostructural nature of Fe_3O_4. It can be seen from the loops in Figures 4a–c that the saturation magnetization (MS) of Fe_3O_4, $Fe_3O_4@SiO_2$, and $Fe_3O_4@SiO_2/[Mn_2L(HL)(H_2O)_4]$ was 66.35, 53.51, and 47.67 emu/g, respectively. Although the mass saturation magnetization in the last 2 composites decreased due to the contribution of the nonmagnetic silica shell and functionalized groups,[25] they still could be efficiently separated from solution media with a permanent magnet.

The decrease in size of MNPs and/or the increase in mass of the monolayer that was nonmagnetic on them may have reduced saturation magnetization.[25] This can be interpreted either by the occurrence of a dead magnetic layer originated by the demagnetization of the surface spins[26] or disordered a spin structure at the surface.[27,28]

When particle size decreases, the ratio of surface to total number of spins increases, which makes the contribution of surface spins to overall magnetization considerable. The super-exchange interaction between Fe–O–Fe ions weakens and the total magnetization of the particle decreases if the surface spins are disordered or misaligned. Additionally, it was established that the saturation magnetization became lower owing to the

high molecular weight of complex. This may be explained by the high molecular weight of complex thickening the coating layer, which lowers the content of Fe_3O_4.[29]
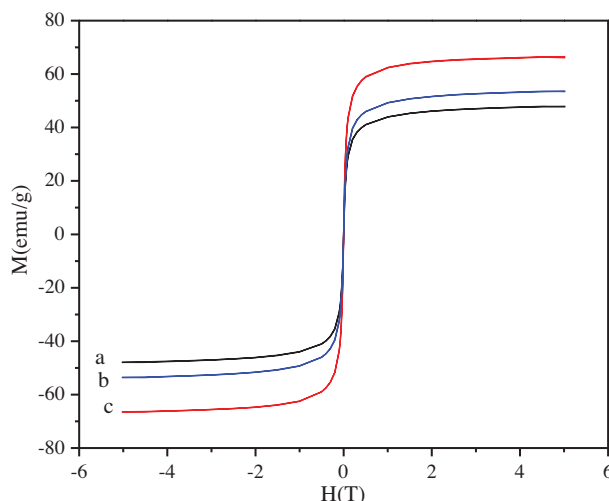
Figure 4. Hysteresis loops of a) $Fe_3O_4@SiO_2/[Mn_2L(HL)(H_2O)_4]$, b) $Fe_3O_4@SiO_2$, c) Fe_3O_4.

2.3. Catalytic activity studies

The catalytic activity of the catalyst was checked for oxidation of sulfides and hydrocarbons with 30% aqueous H_2O_2.

In these reactions, H_2O_2 should be used carefully, due to the possibility of overoxidation.[30] The effect of different amounts of H_2O_2 was investigated with a fixed amount of substrate (1.0 mmol) and catalyst $Fe_3O_4@SiO_2/([Mn_2L(HL)(H_2O)_4]$ (6.4 mg, 0.0016 mmol) in 3 mL of CH_3CN at 60 ± 1 °C.

For sulfoxidation, as shown in Table 1 (entries 1–3), the conversion and selectivity drastically increased with the molecular ratio of H_2O_2 to methyl phenyl sulfide, until the ratio was equal to 3. The catalytic oxidation gave 75% sulfoxide with 3 mmol of H_2O_2 in 60 min (Table 1, entry 3). The excess H_2O_2 required in this catalytic system can be attributed to its decomposition in the presence of the catalyst.[20]

In control experiments without the catalyst, the yield of sulfoxide was low (Table 1, entry 4). Furthermore, when the catalyst was replaced by $Fe_3O_4@SiO_2$, extensive peroxide decomposition was observed and no sulfoxide was obtained (Table 1, entry 5).

Next, the catalytic oxidation was studied in various solvents (Table 2). The catalytic activity decreases in the order acetonitrile (dielectric constant $\varepsilon/\varepsilon_0 = 37.5$) > methanol (32.7) > chloroform (5.5) at 60 °C. Chloroform is not miscible with aqueous H_2O_2, which could also be the reason for low catalytic efficiency. However, the best performance of the catalyst was observed in acetonitrile, which is therefore the solvent of choice. The oxidation was significantly influenced by the reaction temperature (Table 3, entries 1–3). The optimum results were obtained at 60 °C; higher temperatures gave lower yields (Table 3, entry 3). It seems likely that higher temperatures facilitate the decomposition of H_2O_2.[31]

A variety of salen complexes[32] are able to catalyze the oxidation of sulfides to sulfoxides with H_2O_2, but a drawback of these systems is often the use of chlorinated solvents or anhydrous H_2O_2 in ethanol as well as overoxidation to sulfones.

Table 1. Oxidation of methyl phenyl sulfides by the $Fe_3O_4@SiO_2/([Mn_2L(HL)(H_2O)_4]/H_2O_2$.

No.	Substrate	Sulfoxide/Sulfone yield (%)	H_2O_2:Substrate molar ratio	Sulfoxide selectivity (%)[c]
1		23:4	1:1[a]	91
2		52:0	2:1[a]	100
3		75:0	3:1[a]	100
4		11:25	3:1[d]	30
5		0	3:1[e]	—

[a] Reaction conditions: catalyst 6.4 mg (0.0016 mmol), MeSPh 1 mmol, CH_3CN 3 mL, temperature 60 ± 1 °C, time 60 min, [b] Conversions are based on the starting substrate; [c] sulfoxide selectivity: %sulfoxide/(sulfoxide + sulfone); [d] Without catalyst; reaction temperature 60 °C, MeSPh 1.0 mmol, CH_3CN 3 mL, reaction time 2 h, H_2O_2 3 mmol; [e] $Fe_3O_4@SiO_2$ (0.0016 mmol), MeSPh 1.0 mmol, CH_3CN 3 mL, time 2 h, temperature 60 ± 1 °C.

Table 2. Solvent effect on the oxidation of methyl phenyl sulfide with $Fe_3O_4@SiO_2/([Mn_2L(HL)(H_2O)_4]/H_2O_2$.[a]

Entry	Solvent	Conv. (%)[b]	Sulfoxide selectivity (%)[c]
1	$CHCl_3$	13	100
2	CH_3OH	63	100
3	CH_3CN	75	100

[a] Reaction conditions: catalyst 6.4 mg (0.0016 mmol), MeSPh 1.0 mmol, solvent 3 mL, H_2O_2 3 mmol, time 60 min, temperature 60 ± 1 °C; [b] Conversions are based on the starting substrate; [c] sulfoxide selectivity: %sulfoxide/(sulfoxide + sulfone).

Table 3. Temperature effect on the oxidation of methyl phenyl sulfide with $Fe_3O_4@SiO_2/([Mn_2L(HL)(H_2O)_4]/H_2O_2$.[a]
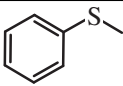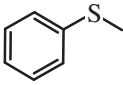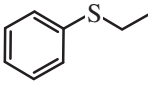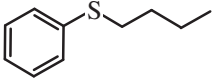
Entry	Temp (°C)	Conv. (%)[b]	Sulfoxide selectivity (%)[c]
1	25	11	100
2	60	75	100
3	80	66	92

[a] Reaction conditions: catalyst 6.4 mg (0.0016 mmol), MeSPh 1.0 mmol, CH_3CN 3 mL, H_2O_2 3 mmol, time 60 min; [b] Conversions are based on the starting substrate; [c] sulfoxide selectivity: %sulfoxide/(sulfoxide + sulfone).

Comparison of the homogeneous and heterogeneous (nanomagnetic and bulk silica gel particles) systems reveals that the heterogeneous catalysts exhibit lower activity than the homogeneous catalyst (Table 4, entries 1, 2). It seems likely that the use of a supported manganese catalyst in the present case gives rise to additional

problems related to the probable dismutation of H_2O_2 by the inorganic support. This would explain why only a few systems based on supported manganese catalysts and H_2O_2 have been reported for oxidation reactions.[33] Related difficulties were earlier encountered for Mn(III)– and Mo(IV)–salen complexes immobilized on mesoporous silica gel.[34]

Table 4. Oxidation of alkyl phenyl sulfides by the $Fe_3O_4@SiO_2/([Mn_2L(HL)(H_2O)_4]/H_2O_2$ and comparing catalytic activity of $Fe_3O_4@SiO_2/([Mn_2L(HL)(H_2O)_4]$ and $[Mn_2L(HL)(H_2O)_4]$ in MeSPh oxidation.

No.	Substrate	Sulfoxide/Sulfone yield (%)[b]	H_2O_2:Substrate molar ratio	Sulfoxide selectivity (%)[c]
1		75:0	3:1[a]	100
2		95:0	3:1[d]	100
3		23:0	3:1[a]	100
4		34:0	3:1[a]	100

[a] Reaction conditions: catalyst 6.4 mg (0.0016 mmol), RSPh 1 mmol, CH_3CN 3 mL, temperature 60 ± 1 °C, time 60 min; [b] Conversions are based on the starting substrate.; [c] sulfoxide selectivity: %sulfoxide/(sulfoxide + sulfone); [d] Reaction conditions: Homogeneous catalyst 1 mg, MeSPh 1 mmol, CH_3CN 3 mL, temperature 60 ± 1 °C, time 120 min.

Table 4 shows that the homogeneous complex in solution was more active for sulfide oxidation than the immobilized counterparts with an equivalent quantity. The lower activity of the anchored complexes may be due to diffusion problems associated with the supports. However, activity and chemoselectivity of $Fe_3O_4@SiO_2/([Mn_2L(HL)(H_2O)_4]$ were higher than those of $SiO_2/([Mn_2L(HL)(H_2O)_4]$. This may be related to the nanoparticle nature of the $Fe_3O_4@SiO_2/([Mn_2L(HL)(H_2O)_4]$ with high specific surface area, which in turns increases the catalytic activity and selectivity.[35] Similar results have been reported by Tangestaninejad et al.; the catalytic activity of [Mn(salophen)Cl] supported on the polystyrene was lower than that on MWCNT nanoparticles[35] and Mn(TPyP)/SiO2–Fe_3O_4 was a much more efficient catalyst than polystyrene-bound Mn(TPyP)OAc.[36]

In this catalytic system, the activity of the heterogeneous $Fe_3O_4@SiO_2/([Mn_2L(HL)(H_2O)_4]$ catalyst is lower than that of the homogeneous $[Mn_2L(HL)(H_2O)_4]$ one, which can be attributed to diffusion problems associated with the supports. Anyway, the activity of heterogeneous $Fe_3O_4@SiO_2/([Mn_2L(HL)(H_2O)_4]$ catalyst is higher than those of similar homogeneous manganese complexes such as biotinylated manganese–salen complexes for aqueous sulfoxidation by using H_2O_2 as an oxidant.[37]

The oxidation of further sulfides was carried out under optimized conditions (Table 4, entries 3, 4). Ethyl phenyl sulfide and n-butyl phenyl sulfide were oxidized by catalyst/H_2O_2 to the corresponding sulfoxides; for these 2 substrates the oxidation yields (23% and 34%, respectively) were lower than the methyl phenyl sulfide oxidation (75%). This can be related to their high steric hindrance.

Finally, it is notable that our catalytic system (catalyst/H_2O_2) is simple and efficient for oxidation of sulfides in comparison with other Mn catalysts,[35,38,39] because our catalytic system shows high conversion without using other additive materials like co-catalysts.

The activities of the catalyst were also tested for the oxidation of toluene, cyclohexane, and ethyl benzene, because oxidations of alkylbenzenes are important transformations in chemical synthesis.[40] In many cases of alkylbenzene oxidation, selectivity is low because of the formation of various by-products. For example, it has been reported that the oxidation of toluene leads to the formation of benzaldehyde, benzyl alcohol, cresols, and benzoic acid because of oxidations of the methyl group and/or of the aromatic ring.[41] Thus, the design of an efficient process for the selective oxidation of alkylbenzenes appears to be an important task.

In order to achieve suitable reaction conditions for maximum transformation of toluene as well as better selectivity for the formation of benzaldehyde, the effects of H_2O_2 concentration (mole of H_2O_2 per mole of toluene), catalyst amount, and temperature were studied.

The effect of H_2O_2 concentration on the toluene oxidation reaction is shown in Table 5. Benzaldehyde was formed as the major product, while benzyl alcohol and benzoic acid were generated as minor ones. No oxidation of the aromatic ring was observed. Four different molar ratios of H_2O_2 to toluene were used (1:1, 2:1, 3:1, and 4:1 mol) in which the amount of toluene was kept fixed at 1 mmol in 3 mL of MeCN (Table 5, entries 1–4). The percentage toluene conversion increased with the increment in H_2O_2 to toluene ratio, until the ratio was equal to 3. The catalytic oxidation gave 21% conversion with good selectivity to benzaldehyde (80%), with 3 mmol of H_2O_2 in 2 h (Table 5, entry 3). However, with ratios higher than 3:1, the excess amount of H_2O_2 caused low selectivity to benzaldehyde, 72.4%, and caused 20.7% and 6.9% selectivity to benzyl alcohol and benzoic acid (Table 5, entry 4), respectively.

Table 5. Effect of oxidant/substrate molar ratio on toluene oxidation.[a]

Entry	H_2O_2: Substrate molar ratio	Conversion.[b](%)	Selectivity(%)	
			Benzaldehyde	Benzyl alcohol
1	1:1	7	57	43
2	2:1	15	76.5	23.5
3	3:1	21	80	20
4	4:1	29	72.4	20.7[c]
5[d]	3:1	3	54	46
6[e]	3:1	0	—	—

[a] Reaction conditions: Fe_3O_4@SiO_2/([Mn_2L(HL)(H$_2$O)$_4$] (0.0016 mmol), toluene 1.0 mmol, CH_3CN 3 mL, time 2 h, temperature 60 $\pm$ 1 °C, [b] Conversions are based on the starting substrate, [c] The other product is benzoic acid, [d] Without catalyst; reaction temperature 60 °C, toluene 1 mmol, CH_3CN 2 mL, reaction time 2 h, H_2O_2 3 mmol; [e] Fe_3O_4@SiO_2 (0.0016 mmol), toluene 1.0 mmol, CH_3CN 3 mL, time 2 h, temperature 60 $\pm$ 1 °C.

A previous study on the catalytic transformation of toluene by t-BuOOH in the presence of Mn(salen) demonstrated that the catalyst immobilized on the polymeric membrane exhibited a slightly lower activity than the unsupported catalyst.[42] The addition of an acid promoter was reported to lead to much higher activity and selectivity for both Mn(salen) and Mn(salen)-PM.[42]

In control experiments, the same as sulfoxidation, without the catalyst, the yield of oxidation was low (Table 5, entry 5). Furthermore, when the catalyst was replaced by Fe_3O_4@SiO_2, due to peroxide decomposition no toluene oxidation was achieved (Table 5, entry 6).

The amount of catalyst has a significant effect on the oxidation of toluene. Five different amounts of catalyst, viz., 12, 14, 16, 18, and 20 ($\times 10^{-4}$ mmol), were used, with all other reaction parameters fixed: namely temperature (60 °C), toluene (1 mmol) to H_2O_2 (3 mmol), and reaction time (2 h). The results are shown in Table 6, entries 1–5, indicating 5%, 13%, 21%, 30%, and 24% conversion corresponding to 12, 14, 16, 18, and 20 $\times 10^{-4}$ mmol catalyst, respectively. The lower conversion of toluene into aldehyde with 12 $\times 10^{-4}$ and 14 $\times 10^{-4}$ mmol catalyst may be because of fewer catalytic sites.[9] The maximum percentage conversion was observed with 18 $\times 10^{-4}$ mmol catalyst, but a further increase of catalyst to 20 $\times 10^{-4}$ mmol resulted in lower conversion, because of adsorption/chemisorption of the 2 reactants on separate catalyst particles, thus reducing the chance to interact.[36,43,44] There was also a sharp decrease in the selectivity to benzaldehyde as the catalyst amount increased to 0.0018 mmol. Beyond 0.0018 mmol catalyst, the conversion obviously declined, which indicated that the excess catalyst can accelerate rapid decomposition of H_2O_2, limiting further oxidation of toluene.[45]

Table 6. Effect of catalyst amount on toluene oxidation.[a]

| Entry | Temp (°C) | Time (h) | Conversion (%) | Selectivity (%) | |
				Aldehyde	Alcohol
1	12	3	5	70	30
2	14	3	13	76	24
3	16	2	21	80	20
4	18	2	20	82	18
5	20	2	24	62.5	37.5

Reaction conditions: a) catalyst $Fe_3O_4@SiO_2/([Mn_2L(HL)(H_2O)_4]$; reaction temperature 60 ± 1 °C, toluene 1 mmol, CH_3CN 3 mL, H_2O_2 3 mmol.

Temperature also had a remarkable effect on the conversion of toluene in the range from 25 to 60 °C; also the aldehyde selectivity strongly depended on the temperature. The conversion of toluene increased with increasing reaction temperature from 25 to 80 °C (Table 7, entries 1–3). Beyond 60 °C, the conversion slightly decreased (Table 7, entry 3). This was possibly caused by acceleration of H_2O_2 decomposition at higher temperature. As a main product of toluene oxidation, the selectivity to benzaldehyde was rapidly declined, while the selectivity to other products such as benzyl alcohol and benzoic acid was increased with the rising temperature. As the temperature rose, the consumed rate of benzaldehyde exceeded its generating rate and the generating rate of benzyl alcohol was faster than that of its conversion into benzaldehyde at higher temperature. However, the benzaldehyde consumption led to an increase in the amount of benzoic acid.[9]

Table 7. Temperature effect on the oxidation of toluene with $Fe_3O_4@SiO_2/([Mn_2L(HL)(H_2O)_4]/H_2O_2$.[a]

| Entry | Temp (°C) | Conversion (%)[b] | Selectivity (%) | |
			Aldehyde	Alcohol
1	25	7	42.8	57.2
2	60	30	82	18
3	80	19	52.6	31.6[c]

[a] Reaction conditions: catalyst (0.0018 mmol), toluene 1.0 mmol, CH_3CN 3 mL, H_2O_2 3 mmol, time 2 h. [b] Conversions are based on the starting substrate; [c] The other product is benzoic acid.

The oxidation of ethyl benzene and cyclohexane was carried out under optimized conditions.

The oxidation takes place on the side chain of ethylbenzene and the results of the % conversion of ethylbenzene (38%) and % selectivity to acetophenone (92%) and benzaldehyde (8%) are presented in Table 8, entry 2. According to the results, the selectivity of catalyst to acetophenone is higher than to the other products, possibly due to the fact that the rate of acetophenone production was greater than that of benzaldehyde production since dehydration is easier than the elimination of methanol. Therefore, the amount of benzoic acid production was trace.[45]

Table 8. Oxidation of hydrocarbons by the $Fe_3O_4@SiO_2/([Mn_2L(HL)(H_2O)_4]/H_2O_2^a$ and $[Mn_2(HL)_2(H_2O)_4]$.[b]

Entry	Hydrocarbon	Conversion (%)[b] (heterogeneous/homogeneous)	Selectivity (%) (heterogeneous/homogeneous)	
1	Toluene	30/42	$82/62^f$	$18/31^g0/7^h$
2	Ethylbenzene	38/50	$92/76^i$	$8/16^f0/8^h$
3	Cyclohexane	24/35	$79.2/57.2^d$	$20.8/42.8^e$

[a] Reaction conditions: Heterogeneous catalyst (0.0018 mmol), alkane 1.0 mmol, CH_3CN 3 mL, H_2O_2 3 mmol, temperature 60 ± 1 °C, time 2 h; [b] Reaction conditions: Homogeneous catalyst (0.0018 mmol), alkane 1.0 mmol, CH_3CN 3 mL, H_2O_2 3 mmol, temperature 60 ± 1 °C, time 3 h; [c] Conversions are based on the starting substrate for heterogeneous/homogeneous conditions [d] The product is cyclohexanone; [e] The product is cyclohexanol; [f] The product is benzaldehyde [g] The product is benzylalcohol; [h] The product is benzoic acid; [i] The product is acetophenone.

In this work, in the oxidation of cyclohexane, an overall conversion of 24% was observed, with 79% selectivity to cyclohexanol and 21% to cyclohexanone (Table 8, entry 3). In this respect, the activity and/or selectivity of this catalyst is much better than that of Mn(III)salophen and Mn(III)salophen-PSI.[46]

Comparison of the homogeneous and heterogeneous systems reveals that the heterogeneous catalysts exhibited lower activity than the homogeneous catalyst (Table 8, entries 1–3). It seems likely that the use of a supported manganese catalyst in the present case gives rise to additional problems related to the probable dismutation of H_2O_2 by the inorganic support. However, it is notable that our heterogeneous catalyst showed higher selectivity than its homogeneous counterpart (Table 8, entries 1–3).

Various homogeneous and heterogeneous Mn catalysts have been used for the oxidation of cycloalkanes with H_2O_2 and t-BuOOH.[47,48] However, none of the reported catalysts showed such high activity and/or selectivity as $[Mn_2(HL)_2(H_2O)_4]$ or $Fe_3O_4@SiO_2/[Mn_2L(HL)(H_2O)_4]$.

2.4. Proposed mechanism for the oxidation of ethylbenzene with H_2O_2 over the $Fe_3O_4@SiO_2/$ $[Mn_2L(HL)(H_2O)_4]$

The mechanism for the oxidation of ethylbenzene with H_2O_2 over the $Fe_3O_4@SiO_2/[Mn_2L(HL)(H_2O)_4]$ catalyst proceeded in several steps as shown in Scheme 2. H_2O_2 was activated by coordinating with the immobilized Mn(II)–Schiff base complexes, that is, the activated distant oxygen of co-coordinated H_2O_2 reacted with ethylbenzene to yield the products. This type of intramolecular hydrogen bond prevents unproductive decomposition of H_2O_2. A similar η^1-hydroperoxide intermediate and formation of 2 products by 2 parallel ways have been assumed for various complexes.[49−51] The structure of the active species for oxidation of ethylbenzene is different from that for the decomposition of H_2O_2. The active species for decomposition of H_2O_2 has a dimeric $(\mu - \eta^1 : \eta^1$-peroxo) dimanganese(III) structure;[52] this conclusion was supported

by other works.[53,54] Ito et al. suggested that there may be another peroxide adduct in the solution of H_2O_2 and it has η^1 coordination mode,[55] as shown in Scheme 3. Since the oxidation of ethylbenzene with the $Fe_3O_4@SiO_2/[Mn_2L(HL)(H_2O)_4]/H_2O_2$ system was decreased by the presence of a 10 equiv. radical scavenger hydroquinone, it was concluded that the breaking of the oxidation of the ethylbenzene with H_2O_2 is supposed to occur by free radical mechanism, yielding primarily ethylbenzene hydroperoxide. A simplified pathway for the oxidation of ethylbenzene by H_2O_2 in the presence of Mn complex is shown in Scheme 4.
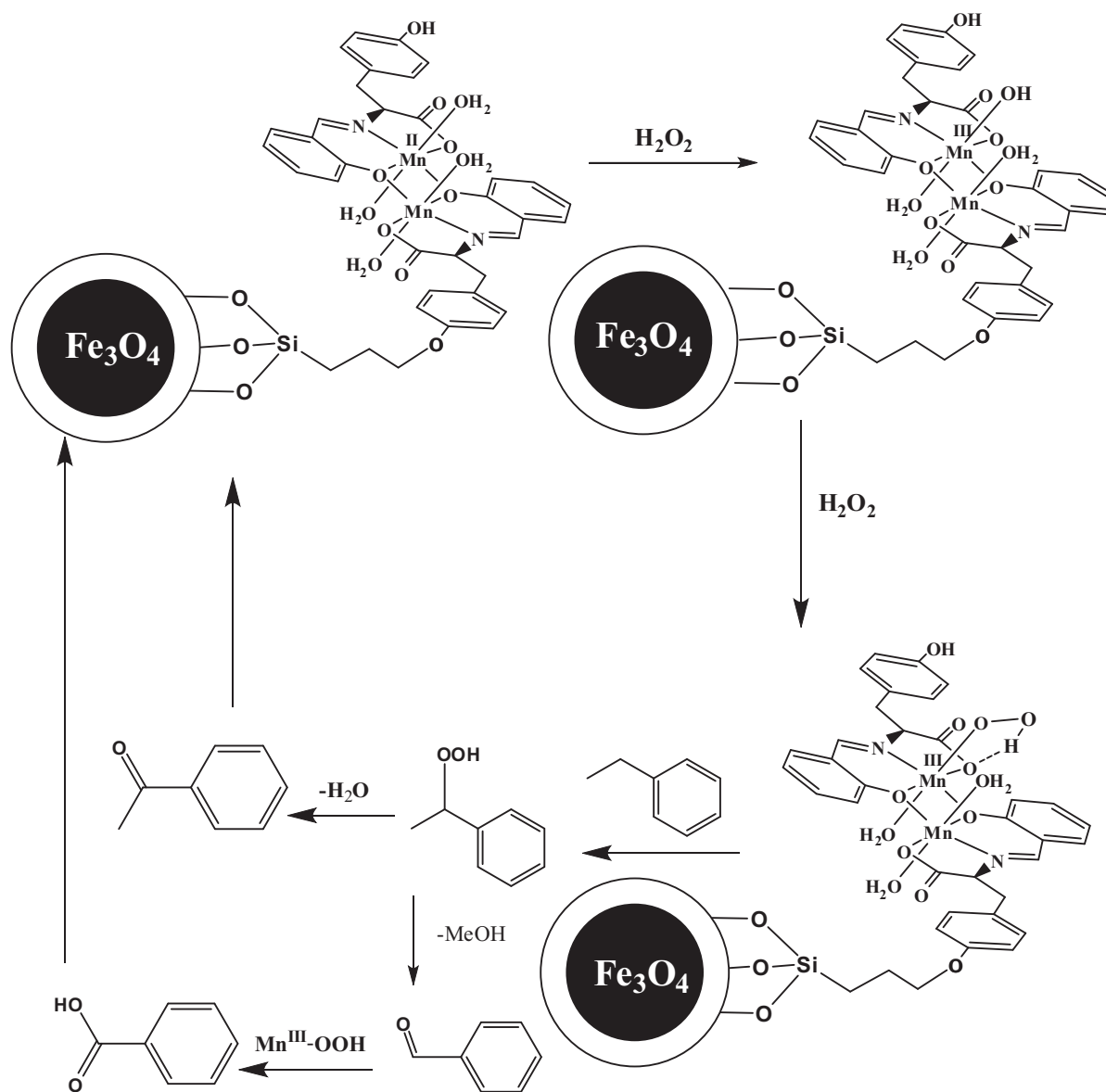
Scheme 2. Proposed mechanism for the oxidation of ethyl benzene with H_2O_2 over $Fe_3O_4@SiO_2$/complex.
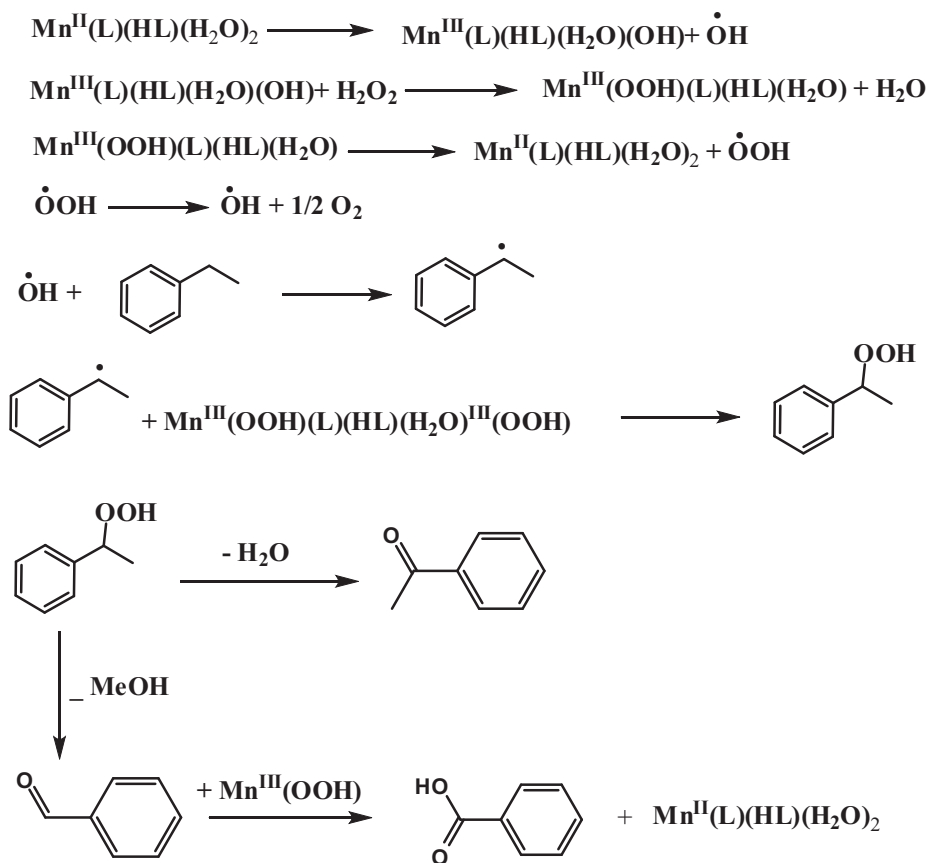
2.5. Catalyst recycling

As reported previously,[3] the catalyst including Fe_3O_4 can be separated from the reaction mixture by a magnet without loss of the catalyst. The recovery and reusability of $Fe_3O_4@SiO_2/[Mn_2L(HL)(H_2O)_4]$ catalyst were
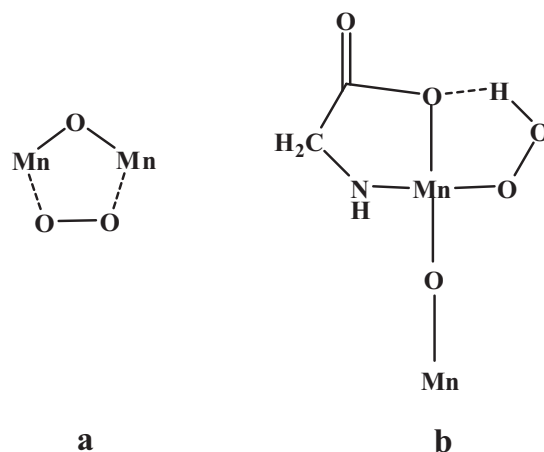
a ($\mu - \eta^1 : \eta^1$-peroxo) dimanganese(III) , b η^1 coordination mode.

Scheme 3. Proposed intermediate for a) oxidation reaction and b) decomposition of H_2O_2.

Scheme 4. Simplified pathway for the oxidation of ethylbenzene by H_2O_2 in the presence of Mn complex.

investigated by the oxidation of methyl phenyl sulfide as a model reaction. Catalyst recycling experiments were carried out by fixing the catalyst magnetically at the bottom of the flask and the solution was decanted after each run. The solid left was washed with MeCN twice, and fresh substrate dissolved in MeCN was introduced into the flask, allowing the system to proceed for the next run. The catalyst was reused 5 times without any

perceptible loss of its catalytic activity, as shown in Table 9. ICP-AES analysis showed that no leaching was observed on the solution phase in the next runs. This catalyst has some remarkable features including ease of separation by an external magnet and, in contrast to other reported similar catalysts, no regeneration process is required after each reaction.[56]

Table 9. Effect of $Fe_3O_4@SiO_2[([Mn_2L(HL)(H_2O)_4]$ catalyst recycling on sulfoxidation.[a]

Number of recycles	Conversion (%)	Selectivity to sulfoxide
Fresh	75	100
1	73	100
2	72	100
3	74	100
4	71	100
5		100

[a] Reaction conditions: a) catalyst $Fe_3O_4@SiO_2/([Mn_2L(HL)(H_2O)_4])$ (0.0018 mmol catalyst); methyl phenyl sulfide 1 mmol, CH_3CN 2 mL, temperature 60 ± 1 °C, reaction time 1 h, H_2O_2 3 mmol.

3. Conclusions

In summary, the present study has described the immobilization of $[Mn_2(HL)_2(H_2O)_4]$ onto a modified magnetic nanoparticle surface. A range of characterization techniques confirm that the metal complex is attached to the magnetic nanoparticle support. $Fe_3O_4@SiO_2/([Mn_2L(HL)(H_2O)_4]$ provides heterogeneous catalysts for oxidation of sulfides and hydrocarbons by H_2O_2. Several factors such as amount of oxidant, type of solvents, and temperature of the reaction mixture affect the performance of this catalyst, and acetonitrile is the solvent of choice. The supported catalyst $Fe_3O_4@SiO_2/([Mn_2L(HL)(H_2O)_4])$ gave low activity compared to its homogeneous counterpart but it has higher activity and selectivity than bulk particles. Thus, the immobilized catalyst could be easily recovered by easy magnetic decantation and reused at least 5 times without noticeable loss of activity. This system could be useful for many other base-catalyzed oxidations.

4. Experimental

4.1. Materials and equipment

The starting materials and solvents were purchased from Merck and used as received. Aqueous 30% H_2O_2 (10.9 mol/L) was used and its exact concentration was determined before use by titration with standard $KMnO_4$. Elemental analyses were conducted on a CHN PerkinElmer 2400 analyzer. FTIR spectra were recorded on a PerkinElmer 597 spectrometer. Manganese content was determined by an inductively coupled plasma–atomic emission spectrometer (ICP-Spectro Genesis). Magnetic measurements were performed on an MPMS XL7 magnetometer. A scanning electron micrograph of the MNPs was taken on a Philips XL 30 SEM instrument. The reaction products of the oxidation were analyzed by an HP Agilent 6890 gas chromatograph, equipped with an HP-5 capillary column (phenyl methyl siloxane 30 m $\times$ 320 μm $\times$ 0.25 μm) with a flame-ionization detector.

4.2. Synthesis of Schiff base ligand (H_3L)

Salicylaldehyde (0.244 g, 2.0 mmol) was dissolved in 10 mL of toluene and to this was added a mixture of L-tyrosine (0.36 g, 2.0 mmol) and NaOH (0.08 g, 2.0 mmol) in 10 mL of toluene. The reaction mixture thus

obtained was refluxed for 2 h and then the resulting yellow solid was filtered, washed with methanol, and dried to give the product, yield 88.0%. IR (KBr, cm^{-1}): 3208 (w) (O–H), 3026 (w), 2963 (w), 2930 (w), 1613 (vs) (C=N), 1514 (m), 1455 (m), 1364 (m), 1332 (s), 1245 (s), 1100 (m), 842 (s), 740 (m), 650 (s), 576 (s), 530 (s), 493 (w), 434 (w).

4.3. Synthesis of the complex

The complex was synthesized according to our previous report.[20] For this purpose, a mixture of L-tyrosine (0.36 g, 2.0 mmol) and NaOH (0.08 g, 2.0 mmol) in CH_2Cl_2 (10 mL) was added to a solution of salicylaldehyde (0.244 g, 2.0 mmol) in CH_2Cl_2 (10 mL) and refluxed, whereupon the colorless solution rapidly turned yellow. The mixture was refluxed for 2 h; then $Mn(OAc)_2 \cdot 4H_2O$ (2 mmol, 0.498 g) was added and the mixture was stirred under reflux for 5 h. The light green precipitate was collected and washed with methanol and dried in air. Yield: 0.5 g (67%). IR (KBr, cm^{-1}): 3424 (br), 3077 (w), 3035 (w), 2921 (m), 2854 (w), 1648 (vs), 1589 (vs), 1549 (w), 1515 (m), 1471 (s), 1444 (s), 1385 (s), 1280 (m), 1187 (m), 823 (m), 757 (s), 526 (m), 449 (m).

4.4. Synthesis of magnetite nanoparticles

Magnetic nanoparticles, Fe_3O_4, were prepared using the procedure reported by Wang et al.[43] Briefly, 0.04 mol of $FeCl_3 \cdot 6H_2O$ and 0.02 mol of $FeCl_2 \cdot 4H_2O$ were dissolved in 50 mL of 0.5 M HCl solution, which was then added dropwise to 500 mL of 1.5 mol/L sodium hydroxide solution at 80 °C under a nitrogen flow (40 mL/min) with vigorous stirring. The obtained Fe_3O_4 nanoparticles were repeatedly washed with deionized water followed by drying at 50 °C under vacuum for 4 h. FTIR (KBr, cm^{-1}): 3400 (br), 580 (s).

Silica-coated magnetite nanoparticles ($Fe_3O_4@SiO_2$) were made by sol-gel method.[44] According to these references, the magnetite nanoparticles (0.5 g) were dispersed in ethanol (50 mL). NH_4OH (3 mL) and TEOS (1 mL) were added successively. After stirring for 10 h, the black precipitate was collected with a permanent magnet, and rinsed with ethanol 3 times. The product was dried and stored under vacuum conditions.

FTIR (KBr, cm^{-1}): 3441 (br) (O–H), 1097 (vs), 921 (w), 817 (w), 577 (w), 477 (m), 434 (m).

4.5. Preparation of the supported complex

For immobilization of the complex, firstly we functionalized the $Fe_3O_4@SiO_2$ with a good linker such as CPTMS. The functionalized $Fe_3O_4@SiO_2$/CPTMS was prepared according to Saeedi et al.[36] According to their report, $Fe_3O_4@SiO_2$ nanoparticles (1.0 g) were dispersed in dry toluene (30 mL) by sonication for 1 h. Then 3-chloropropyltrimethoxysilane (1.8 mL, 10 mmol) was added and the reaction mixture was refluxed for 24 h under argon atmosphere. At the end of the reaction, the mixture was cooled to room temperature; the products were adsorbed on a magnet and rinsed twice with dry toluene (100 mL) and twice with dry acetone (100 mL). The obtained particles were dried under vacuum conditions. Linker loading = 1.43 mmol/g MNP silica gel.

Then $Fe_3O_4@SiO_2$/CPTMS (0.5 g) and $[Mn_2(LH)_2(H_2O)_4]$ (0.1 g) were refluxed in CH_2Cl_2 for 24 h and then washed with CH_2Cl_2 for 4 h in order to eliminate all the $[Mn_2(LH)_2(H_2O)_4]$ complexes adsorbed on the support. The brown material, $Fe_3O_4@SiO_2/[Mn_2L(HL)(H_2O)_4]$, was dried at room temperature and characterized by CHN, SEM, ICP, IR spectroscopy, and VSM. Mn loading = 0.50 mmol/g MNP silica gel, Complex loading = 0.25 mmol/g MNP silica gel. FTIR (KBr, cm^{-1}): 3445 (br, w), 2929 (w), 2861 (w), 1647

(s), 1596 (s), 1517 (w), 1471 (m), 1446 (m), 1388 (s), 1088 (vbr, vs), 825 (vs), 758 (m), 684 (w), 577 (s), 472 (s).

4.6. General oxidation procedure

Oxidation reactions were carried out under air at $60 \pm 1\ ^\circ\text{C}$ with acetonitrile as solvent and aqueous 30% H_2O_2 (10.9 M) as oxidant. In a typical experiment, a mixture of 0.0016 mmol of $Fe_3O_4@SiO_2/([Mn_2L(HL)(H_2O)_4]$ as the catalyst, 3.0 mL of solvent, and 1.0 mmol of the sulfide were mixed in a 25-mL glass flask. After the mixture was heated to 60 $^\circ$C, H_2O_2 was added. At appropriate intervals, aliquots were removed and analyzed immediately by GC. The oxidation products were identified by comparing their retention times with those of authentic samples. Yields are based on the added substrate and were determined by a calibration curve.

Acknowledgments

References

1. Wei, Z. J.; Wang C. Y.; Liu, H.; Zou, S. W.; Tong, Z. *Colloids and Surfaces B, Biointerfaces* **2012**, *91*, 97–105.

2. Astruc, D.; Lu, F.; Aranzaes, J. R. *Angew. Chem. Int. Ed.* **2005**, *44*, 7852–7872.

3. Kooti, M.; Afshari, M. *Mater. Res. Bull.* **2012**, *47*, 3473–3478.

4. Dutta, B.; Jana, S.; Bhattacharjee, A.; Gutlich, P.; Iijima, S. I.; Koner, S. *Inorg. Chim. Acta* **2010**, *363*, 696–704.

5. Long, W.; Gill, C. S.; Choi, S.; Jones, C. W. *Dalton Trans.* **2010**, *39*, 1470–1472.

6. Fernandez, I.; Khiar, N. *Chem. Rev.* **2003**, *103*, 3651–3705.

7. Sahoo, S.; Kumar, P.; Lefebvre, F.; Halligudi, S. B. *J. Catal.* **2009**, *262*, 111–118.

8. Punniyamurthy, T.; Velusamy, S.; Iqbal, J. *Chem. Rev.* **2005**, *105*, 2329–2363.

9. Li, X.; Lu, B.; Sun, J.; Wang, X.; Zhao, J.; Cai, Q. *Catal. Commun.* **2013**, doi: 10.1016/j.catcom.2013.05.001.

10. Ghiaci, M.; Molaie, F.; Sedaghat, M.; Dorostkar, N. *Catal. Commun.* **2010**, *11*, 694–699.

11. Valkenberg, M. H.; Holderich, W. F. *Catal Rev.* **2002**, *44*, 321–374.

12. Polshettiwar, V.; Luque, R.; Fihri, A.; Zhu, H.; Bouhrara, M.; Basset, J. M. *Chem. Rev.* **2011**, *111*, 3036–3075.

13. Lim, C. W.; Lee, I. S. *Nano. Today* **2010**, *5*, 412–434.

14. Wang, H.; Huang, J.; Ding, L.; Li, D.; Han, Y. *Appl. Surf. Sci.* **2011**, *257*, 7107–7112.

15. Gill, C. S.; Price, B. A.; Jones, C. W. *J. Catal.* **2007**, *251*, 145–152.

16. Schatz, A.; Reiser, O.; Stark, W. J. *Chem. Eur. J.* **2010**, *16*, 8959–8967.

17. Peng, X.; Wang, Y.; Tang, X.; Liu, W. *Dyes Pigments* **2011**, *91*, 26–32.

18. Qu, L.; Tie, S. *Micropor. Mesopor. Mater.* **2009**, *117*, 402–405.

19. Yan, X.; Chen, J.; Xue, Q.; Miele, P. *Micropor. Mesopor. Mater.* **2010**, *135*, 137–142.

20. Ghorbanloo, M.; Jaworska, M.; Paluch, P.; Li, G. D.; Zhou, L. *J. Transit Met. Chem.* **2013**, DOI: 10.1007/s11243-013-9718-4.

21. Heinert, D, Martell, A. E. *J. Am. Chem. Soc.* **1962**, *84*, 3257–3263.

22. Zhang, X.; Niu, H.; Pan, Y.; Shi, Y.; Cai, Y. *J. Colloid Interface Sci.* **2011**, *362*, 107–112.

23. Neves, A.; Erthal, S. M. D.; Vencato, I.; Ceccato, A. S.; Mascarenhas, Y. P.; Nascimento, O. R.; Horner, M. *Inorg. Chem.* **1992**, *31*, 4749–4751.

24. Dahlan, I.; Lee, K. T.; Kamaruddin, A. H.; Mohamed, A. R.; Hazard, J. *Mater.* **2009**, *166*, 1556–1559.

25. Goya, G. F.; Berquo, T. S.; Fonseca, F. C.; Morales, M. P. *J. Appl. Phys.* **2003**, 94, 3520–3528.

26. Berkowitz, A. E.; Schuele, W. J.; Flanders, P. J. *J. Appl. Phys.* **1968**, *39*, 1261–1263.

27. Kodama, R. H.; Berkowitz, A. E.; McNiff, E. J.; Foner, F. S. *Phys. Rev. Lett.* **1996**, *77*, 394–397.

28. Coey, J. M. D. *Phys. Rev. Lett.* **1971**, *27*, 1140–1142.

29. Zhu, Z.; Wei, X.; Xu, F.; Wang, Y. *Solid State Sci.* **2012**, *14*, 1550–1556.

30. Noyori, R.; Aoki, M.; Sato, K. *Chem. Commum.* **2003**, 1977–1986.

31. Adam, F.; Ooi, W. T. *Appl. Catal. A: Gen.* **2012**, *445–446*, 252–260.

32. Jeong, Y. C.; Choi, S.; Hwang, Y. D.; Ahn, K. H. *Tetrahedron Lett.* **2004**, *45*, 9249–9252.

33. Rao, Y. V. S.; De Vos, D. E.; Bein, T.; Jacobs, P. A. *Chem. Commun.* **1997**, 355–356.

34. Ghorbanloo M.; Hosseini Monfared, H.; Janiak, C. *J. Mol. Catal. A: Chem.* **2011**, *345*, 12–20.

35. Tangestaninejad, S.; Moghadam, M.; Mirkhani, V.; Mohammadpoor-Baltork, I.; Saeedi, M. S. *Appl. Catal. A: Gen.* **2010**, *381*, 233–241.

36. Saeedi, M. S.; Tangestaninejad, S.; Moghadam, M.; Mirkhani, V.; Mohammadpoor-Baltork, I.; Khosropour, A. R. *Polyhedron* **2013**, *49*, 158–166.

37. Pordea, A.; Mathis, D.; Ward, T. R. *J. Organmet. Chem.* **2009**, *694*, 930–936.

38. Ghaemi, A.; Rayati, S.; Zakavi, S.; Safari, N. *Appl. Catal. A: Gen.* **2009**, *353*, 154–159.

39. Lindsay Smith, J. R.; Murray, J.; Waltona, P. H.; Lowdon, T. R. *Tetrahedron Letters* **2006**, *47*, 2005–2008.

40. Hudlicky, M. *Oxidations in Organic Chemistry*, Am. Chem. Soc, Washington, DC, USA, 1990, p. 99.

41. Huang, G.; Luo, J.; Cai, C.; Guo, Y.; Luo, G. *Catal. Commun.* **2008**, *9*, 1882–1885.

42. MacLeod, T. C. O.; Kirillova, M. V.; Pombeiro, A. J. L.; Schiavon, M. A.; Assis, M. D. *Appl. Catal. A: Gen.* **2010**, *372*, 191–198.

43. Wang, J.; Zheng, S.; Shao, Y.; Liu, J.; Xu, Z.; Zhu, D. *J. Colloid Interface Sci.* **2010**, *349*, 293–299.

44. Shokouhimehr, M.; Piao, Y.; Kim, J.; Jang, Y.; Hyeon, T. *Angew. Chem., Int. Ed.* **2007**, *46*, 7039–7043.

45. Habibi, D.; Faraji, A. R. *Appl. Surf. Sci.* **2013**, *276*, 487–496.

46. Mirkhani, V.; Moghadam, M.; Tangestaninejad, S.; Bahramian, B. *Appl. Catal. A: Gen.* **2006**, *311*, 43–49.

47. Nakayama, N.; Tsuchiya, S.; Ogawa, S. *J. Mol. Catal. A: Chem.* **2007**, *277*, 61–71.

48. Jha, R. K.; Shylesh, S.; Bhoware, S. S.; Singh, A. P. *Micropor. Mesopor. Mater.* **2006**, *95*, 154–163.

49. Alavi, S.; Hosseini-Monfared, H.; Siczek, M. *J. Mol. Catal. A: Chem.* **2013**, *377*, 16–28.

50. Habibi, D.; Faraji, A. R. *Appl. Surf. Sci.* **2013**, *276*, 487–496.

51. Arshadi, M.; Ghiaci, M.; Ensafi, a. A.; Karimi-Maleh, H.; Suib. S. L. *J. Mol. Catal. A: Chem.* **2011**, *338*, 71–83.

52. Nishida, Y.; Nasu, M.; Akamatsu, T.; Naturforsch, T. *Z. Naturforsch., Teil B*. **1992**, *47*, 115.

53. Menage, S.; Vincent, J. M.; Lambeaux, C.; Fontecave, M. J. *J. Chem. Soc. Dalton Trans.* **1994**, 2081–2084.

54. Nishida. Y.; Ito, S.; Naturforsch, Z. *Z. Naturforsch., Teil C.* **1995**, SO. 205.

55. Ito, S.; Okuno, T.; Matsushima, H.; Tokii, T.; Nishida, Y. *J. Chem. Soc., Dalton Trans.* **1996**, 4479–4484.

56. Zhang, Z.; Zhang, F.; Zhu, Q.; Zhao, W.; Ma, B.; Ding, Y. *J. Colloid Interface Sci.* **2011**, *360*, 189–194.